nature COMMUNICATIONS

ARTICLE

Received 21 Aug 2012 | Accepted 25 Jan 2013 | Published 26 Feb 2013

DOI: 10.1038/ncomms2546

OPEN

Critical fictive temperature for plasticity in metallic glasses

Golden Kumar[1], Pascal Neibecker[2], Yan Hui Liu[2] & Jan Schroers[2]

A long-sought goal in metallic glasses is to impart ductility without conceding their strength and elastic limit. The rational design of tough metallic glasses, however, remains challenging because of the inability of existing theories to capture the correlation between plasticity, composition and processing for a wide range of glass-forming alloys. Here we propose a phenomenological criterion based on a critical fictive temperature, T_{fc}, which can rationalize the effect of composition, cooling rate and annealing on room-temperature plasticity of metallic glasses. Such criterion helps in understanding the widespread mechanical behaviour of metallic glasses and reveals alloy-specific preparation conditions to circumvent brittleness.

[1] Department of Mechanical Engineering, Texas Tech University, Box 41021, 7th and Boston, Lubbock, Texas 79409, USA. [2] Department of Mechanical Engineering and Materials Science, Yale University, New Haven, Connecticut 06511, USA. Correspondence and requests for materials should be addressed to G.K. (email: golden.kumar@ttu.edu).

Despite their similar inherent amorphous structure, which endows metallic glasses with high strength and elasticity[1–4], they exhibit a broad range of damage tolerance, from ideal brittle to remarkably tough[5–8]. Such wide spectrum of mechanical properties is in stark contrast to oxide glasses, and understanding the origin has been the focus of the metallic glass community for the last decade[6–12]. Mechanical response of a metallic glass is further influenced by extrinsic effects, such as cooling rate[13], sample size[14,15] and testing conditions (temperature and strain rate)[16,17]. Besides these extrinsic factors, the understanding of composition-dependent plasticity in metallic glasses continues to defy proposed theories. For example, Pd-based metallic glass is significantly more brittle compared with Pt-based metallic glass prepared at a similar cooling rate[18]. Plasticity of Zr-Cu-Al metallic glasses is very sensitive to composition, whereas their microstructure and elastic constants are largely unaffected[19,20]. The atomic-level structure underlying this different mechanical response of metallic glasses is difficult to characterize. Computational modelling offers some insight about the composition–structure–property relationship; however, the lowest achievable cooling rates in simulation are still several orders of magnitude higher than experimental cooling rates[11].

Following the analogy from crystalline metals, the toughness of metallic glasses has been correlated with their elastic constants[6,9,21,22]. Higher Poisson's ratio or lower G/B (G: shear modulus, B: bulk modulus) ratio is predicted to result in higher toughness in metallic glasses, mechanistically by increasing the resistance for crack opening compared with shear band formation and extension. Therefore, a high Poisson's ratio or low G/B has been often used as an indicator for designing tough metallic glasses[6,9]. In recent years, increasing experimental evidence has mounted about the limited applicability of G/B in predicting the mechanical response of metallic glasses[18,23–25]. In particular, a marginal change in elastic constants cannot account for the sever annealing-induced embrittlement observed in metallic glasses[23]. These findings suggest that a simple, elastic moduli-based approach does not capture the essential features of the multifaceted plasticity problem in amorphous metals. A comprehensive description for the mechanical behaviour of metallic glasses requires the understanding of the complex interplay between their composition, processing, structure and properties.

In polymer and oxide glasses, it has been widely observed that the properties of a glass at room temperature are reminiscent of its supercooled liquid at the fictive temperature (T_f)[26–28]. For metallic glasses, it has been shown that the room-temperature elastic constants can be directly correlated with the values of the supercooled liquid through the linear Debye-Grüneisen thermal expansion[29]. Therefore, knowledge of the supercooled liquid state and the fictive temperature can provide a key insight about the room-temperature properties of metallic glasses.

In this work, we study the effect of fictive temperature on the room-temperature plasticity of bulk metallic glasses (BMGs). Samples that are brittle at room temperature may deform plastically at higher temperatures as reported earlier[17]. However, the goal of the present study is to understand the room-temperature mechanical response and its correlation with the properties of their supercooled liquids among different glass-forming alloys. Three BMG formers are considered: $Pt_{57.5}Cu_{14.7}Ni_{5.3}P_{22.5}$ (Pt-BMG), $Pd_{43}Cu_{27}Ni_{10}P_{20}$ (Pd-BMG) and $Zr_{44}Ti_{11}Cu_{10}Ni_{10}Be_{25}$ (Zr-BMG). In this study, 2.5% strain to failure is set as the ductile–brittle transition to accommodate ±0.5% measurement error, because even the most brittle metallic glasses still exhibit approximately 2% elastic strain[4]. Our results show that the room-temperature plasticity of BMGs decreases with lowering the fictive temperature, and falls below the ductile–brittle transition at a critical fictive temperature, T_{fc}, which is characteristic of the BMG former. We demonstrate that T_{fc} is a key parameter that defines the mechanical behaviour of BMGs and its sensitivity to cooling rate and annealing.

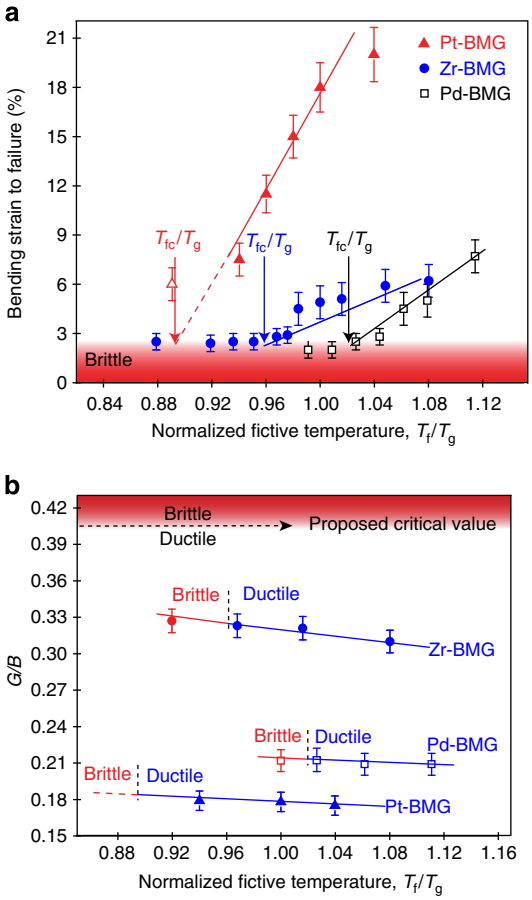

Figure 1 | Effect of fictive temperature on strain and elastic constants. (**a**) Room-temperature bending strain to failure as a function of normalized fictive temperature for Pt-BMG, Zr-BMG and Pd-BMG. The critical fictive temperature for ductile–brittle transition is 0.89 T_g, 0.96 T_g and 1.02 T_g for Pt-BMG, Zr-BMG and Pd-BMG, respectively. The open triangle is the strain to failure for Pt-BMG annealed at 0.89 T_g for 30 days. (**b**) G/B ratio shows a weak dependence on fictive temperature. The G/B ratio for the embrittled BMGs is well below the proposed critical value for ductile–brittle transition.

Results

Bending strain and elastic constants. Room-temperature strain to failure corresponding to different fictive temperatures for the considered BMG formers is shown in Fig. 1a. The temperature scale is normalized to the calorimetric glass transition temperature, T_g, listed in Table 1. A common feature of all three BMGs is that their strain to failure decreases with lowering T_f and it drops below the ductile–brittle transition for $T_f < T_{fc}$. The plastic strain appears to correlate with $T_f - T_{fc}$, which is remarkably similar to the temperature dependence of free volume ($v_f \sim T - T_0$, v_f is free volume and T_0 is Vogel–Fulcher–Tammann temperature) predicted by the Vogel–Fulcher–Tammann equation[30]. Besides this common trend, there are several notable distinctions among three BMGs. The strain to failure for the Pt-BMG remains significantly

Table 1 | Calorimetric T_g measured at a heating rate of 20 K min^{-1}, T_{fc}, $T_g - T_{fc}$ and G/B ratio for the considered BMG formers.

BMG former	T_g (K)	T_{fc} (K)	$T_g - T_{fc}$ (K)	G/B
$Pt_{57.5}Cu_{14.7}Ni_{5.3}P_{22.5}$	503	446	57	0.17
$Pd_{43}Cu_{27}Ni_{10}P_{20}$	568	580	−12	0.21
$Zr_{44}Ti_{11}Cu_{10}Ni_{10}Be_{25}$	623	598	25	0.31

Abbreviations: BMG, bulk metallic glass; G/B, shear modulus/bulk modulus; T_{fc}, critical fictive temperature; T_g, glass transition temperature.
T_{fc} is experimentally determined from the bending plasticity of relaxed samples. G/B is calculated from the ultrasonic measurements on the as-cast samples.

higher than that for the Zr-BMG and the Pd-BMG after annealing at the same normalized fictive temperatures. The T_{fc} for the Pd-BMG former is highest among considered BMG formers and occurs above calorimetric T_g, whereas for the Zr-BMG former and the Pt-BMG this transition is below T_g. Figure 1b shows the variation in G/B values as a function of normalized fictive temperature. The G/B values for the as-quenched BMGs are listed in Table 1. The change in G/B with fictive temperature is small even though plasticity changes significantly. For all three BMG formers, the G/B ratio corresponding to the critical fictive temperature T_{fc} is far below that of the previously proposed lower limit of 0.41 for brittleness[9].

Thermal embrittlement of metallic glasses, as displayed in Fig. 1a, is typically attributed to reduction in free volume through structural relaxation[31,32]. The structural relaxation time at T_g is approximately 100 s and increases exponentially with decreasing temperature[33]. At temperature far below T_g, it is impractical to attain completely relaxed glassy state. This suggests that a metallic glass exhibiting T_{fc} far below T_g should not become brittle during experimental annealing time. To test this correlation, Pt-BMG was annealed for 30 days at its estimated T_{fc} of 446 K, which is 57 K below the T_g. The sample remained ductile and displayed a bending strain of 6% (open triangle in Fig. 1a). According to the relaxation kinetics, it would take about 30 years to structurally relax Pt-BMG at 446 K (ref. 34). In contrast, the Zr-BMG with a T_{fc} of only 25 K below its T_g, is sensitive to embrittlement during annealing near T_g (ref. 23). The Pd-BMG is even more susceptible to annealing-induced embrittlement because of its T_{fc} above T_g, which corresponds to a relaxation time of only 50 s. Consequently, the difference between T_g and T_{fc} of a metallic glass correlates with its resistance to annealing-induced embrittlement.

Effect of cooling rate. Mechanical properties of some BMGs strongly depend on the cooling rate during vitrification, whereas others show little or no variation[13,18,21]. The degree of cooling-rate sensitivity among BMG formers can be rationalized based on their T_{fc} values. If the cooling rate is sufficiently fast, the resulting T_f is higher than T_{fc}, and the BMG is ductile. A slower cooling rate will result in lower T_f, and the glassy state will become brittle if T_f drops below T_{fc}. Typical cooling rates that result in bulk metallic glass formation (thickness >1 mm) span over four orders of magnitude ranging from 0.1 to 1,000 K s^{-1} (ref. 35). Experimental measurements in a wide range of glass-forming liquids reveal that T_f decreases by 5–10 K for every order-of-magnitude decrease in cooling rate[28,36,37]. The maximum variation in T_f, as a result of cooling rate, can be approximated to 40 K for BMG formers (Fig. 2). This implies that for a BMG whose T_{fc} differs from its T_f by more than 40 K, its ductile or brittle behaviour will remain essentially unaffected by the cooling rate. BMG formers with $T_f - T_{fc} > 40$ K will be ductile and the ones with $T_f - T_{fc} \leq 40$ K will be brittle for typical cooling rates used in BMG

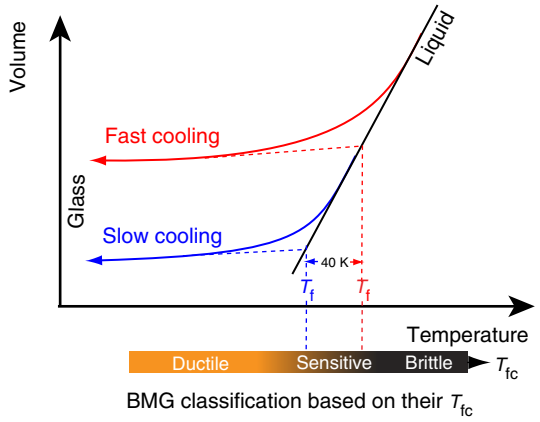

Figure 2 | The predicted mechanical behaviour of BMG formers under typical cooling rates. The maximum variation in T_f is about 40 K as a result of critical cooling rate, which spans over four orders of magnitude among BMG formers. BMG formers with T_{fc} out of the accessible T_f range are either always ductile ($T_f - T_{fc} > 40$ K) or brittle ($T_f - T_{fc} \leq 40$ K). However, BMG formers with $T_{fc} \sim T_f$ can change from ductile–brittle within practical cooling-rate variations.

formation. In contrast, the BMG formers with T_{fc} in the proximity of T_f (Fig. 2) will be sensitive to the cooling rates.

Isothermal embrittlement diagrams. The existence of T_{fc} is experimentally manifested in the cooling-rate-dependent mechanical behaviour of BMGs. Several BMGs such as Fe-based and Mg-based, which are known to be typically brittle, become ductile when cooled at higher rates[21,38]. The cooling rate (R_e) to prevent embrittlement and its relation with the T_{fc} can be understood from isothermal time–temperature–transformation (TTT) diagrams for embrittlement (Fig. 3). The embrittlement time is the annealing time required to decrease the bending strain below the ductile–brittle limit. The embrittlement time decreases with increasing temperature till T_{fc} and then increases abruptly before decreasing again with further increase in temperature. The discontinuity at T_{fc} is related to the change in embrittlement mechanism from structural relaxation ($T \leq T_{fc}$) to crystallization ($T > T_{fc}$). The T_{fc} is the highest temperature at which a metallic glass can embrittle by structural relaxation. Consequently, the embrittlement of a glassy state through relaxation is fastest at T_{fc} that corresponds to the 'nose' of embrittlement curves in Fig. 3. The embrittlement time at the nose, t_e, determines the cooling rate R_e to vitrify a ductile glassy state. The t_e values for Pd-BMG, Zr-BMG and Pt-BMG are 50 s, 5,000 s, and 9E–9 s, respectively. These values scale with the difference $T_g - T_{fc}$ (Pt-BMG > Zr-BMG > Pd-BMG). The short t_e indicates that R_e is highest for Pd-BMG among the considered BMG formers. The critical cooling rate (R_c) for glass formation, however, follows the opposite trend and is lowest (0.09 K s^{-1}) for the Pd-BMG[35]. This suggests that the critical cooling rates for avoiding crystallization and embrittlement are not directly correlated.

Discussion

A comprehensive framework to account for the diverse mechanical behaviour of metallic glasses can be constructed based on the knowledge of $T_f - T_{fc}$. According to this criterion, all metallic glasses can be broadly classified into two groups: $T_f - T_{fc} < 0$ (type I) and $T_f - T_{fc} > 0$ (type II). For type I metallic glasses, the embrittlement nose time is shorter than the crystallization nose time and, consequently, the critical cooling rate to prevent

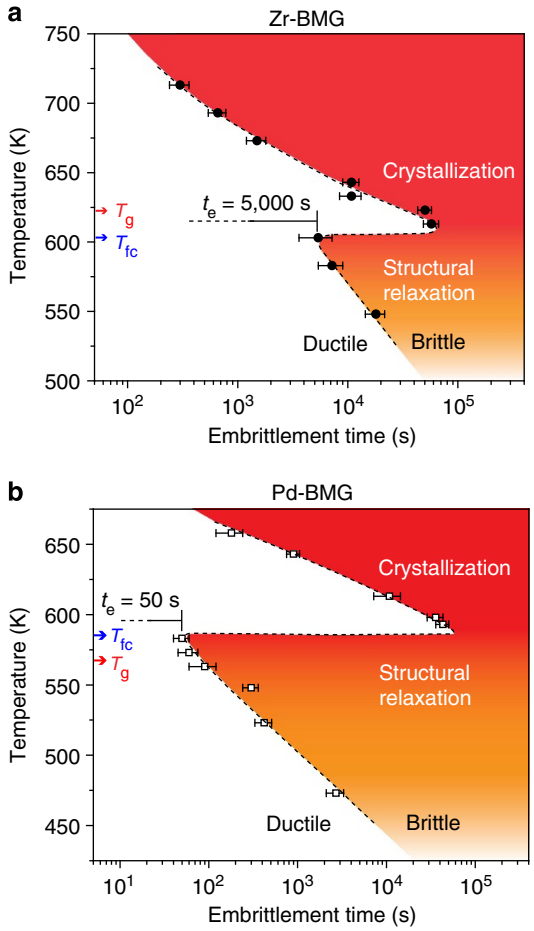

Figure 3 | TTT diagrams for embrittlement. The T_{fc} is the highest temperature where embrittlement can occur owing to structural relaxation. Above T_{fc}, the embrittlement time increases abruptly because of change in origin of embrittlement from structural relaxation to crystallization. The time (t_e) at T_{fc} defines the nose of TTT diagrams for embrittlement. The measured t_e is 5,000 s for Zr-BMG (**a**) and 50 s for Pd-BMG (**b**).

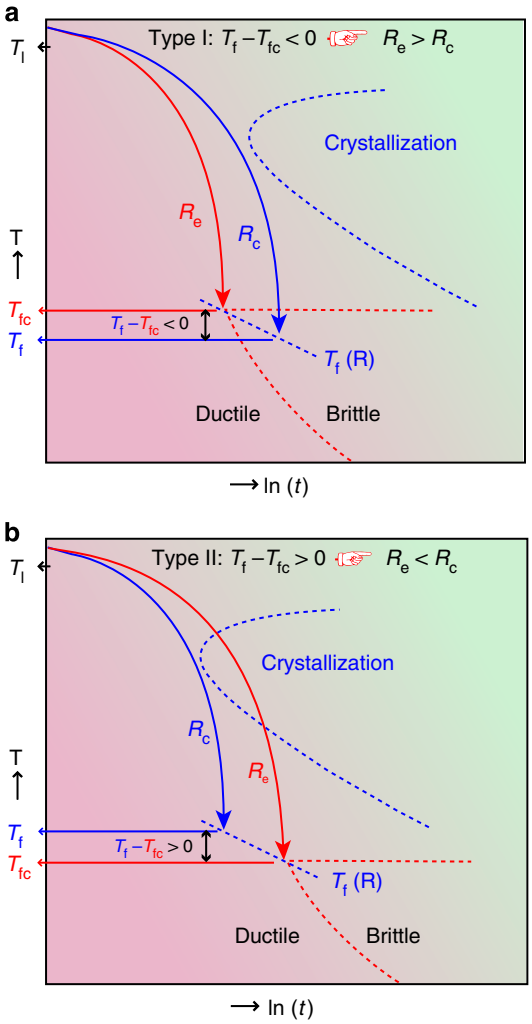

Figure 4 | Classification of BMG formers based on $T_f - T_{fc}$ values. (**a**) Type I metallic glasses ($T_f - T_{fc} < 0$) exhibit an embrittlement nose time shorter than the crystallization nose. As a result, these BMG formers are typically brittle but can be made ductile if a cooling rate higher than R_e is applied. (**b**) For type II metallic glasses ($T_f - T_{fc} > 0$), the embrittlement nose time is longer than the crystallization nose time; therefore, these BMG formers are always ductile. In both cases, variation of T_f with cooling rate is shown. For practical convenience, calorimetric T_g can be used to approximate T_f.

embrittlement is higher than the critical cooling rate for glass formation (Fig. 4a). Here T_f is the fictive temperature of a glass vitrified at its critical cooling rate for glass formation. The magnitude of $T_f - T_{fc}$ determines their mechanical behaviour and its sensitivity to cooling rate and annealing. Metallic glasses with a small negative $T_f - T_{fc}$ are sensitive to preparation conditions and can change from ductile to brittle or vice versa with varying cooling rates. For metallic glasses with large negative $T_f - T_{fc}$, the embrittlement nose time is much shorter than the crystallization nose time. Consequently, their bulk states are always brittle. This explains why Fe-based and Mg-based metallic glasses require high cooling rates, unachievable in bulk form, to vitrify into a ductile state[21].

Type II metallic glasses ($T_f - T_{fc} > 0$) exhibit an embrittlement nose time that is longer than the crystallization nose time (Fig. 4b). Hence, their critical cooling rate for embrittlement is lower than the critical cooling rate for glass formation. These metallic glasses are always ductile in the as-cast bulk state and the magnitude of $T_f - T_{fc}$ indicates their resistance to annealing-induced embrittlement. Metallic glasses with a large positive $T_f - T_{fc}$ (for example, Pt-BMG) do not become brittle under practical annealing conditions, because their embrittlement time ($\approx$relaxation time) at T_{fc} is extremely long. In contrast, metallic glasses with a small positive $T_f - T_{fc}$ (for example, Zr-BMG) are ductile in the as-cast state but are susceptible to annealing-induced embrittlement because of their fast relaxation at T_{fc}.

According to this critical fictive temperature viewpoint, the knowledge of T_{fc} and T_f is sufficient to understand a BMG's resistance to annealing-induced embrittlement, cooling rate sensitivity and critical cooling rate for plasticity. In practice, T_f measured by method of integration from differential scanning calorimeter (DSC) heating curves is typically few degrees lower than the T_g (ref. 39). Therefore, calorimetric T_g values can be used as a good approximation of T_f for the practical application of plasticity criteria outlined here. Our experimental results validate the use of calorimetric T_g for prediction of mechanical response of BMG formers. Pt-BMG with $T_g - T_{fc} \sim 57$ K is ductile at any cooling rate and exhibits higher resistance to annealing embrittlement. Zr-BMG with $T_g - T_{fc} \sim 25$ K is ductile in the as-cast state, but becomes brittle during sub-T_g annealing[23].

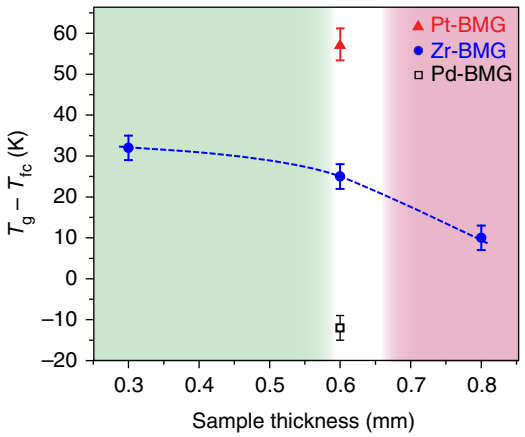

Figure 5 | Effect of sample size on the critical fictive temperature. $T_g - T_{fc}$ values for Zr-BMG of different thicknesses are compared with that of 0.6-mm thick Pt-BMG and Pd-BMG samples. The results demonstrate that the effect of alloy composition is more pronounced than sample size. Therefore, T_{fc} measured for any sample size can be used in the $T_g - T_{fc}$ criterion for plasticity.

Pd-BMG with $T_g - T_{fc} \sim -12$ K changes from ductile to brittle when the cooling rate is decreased below 50 K s^{-1} (ref. 18).

The absolute values of T_{fc} and hence $T_g - T_{fc}$ are a function of sample size because of the size-dependent plasticity of BMGs[13,15]. Figure 5 shows $T_g - T_{fc}$ for Zr-BMG samples of different thicknesses. $T_g - T_{fc}$ increases with decreasing temperature. However, this size dependence is much smaller than the effect of composition on $T_g - T_{fc}$. For Pt-BMG of 0.6 mm thickness, the $T_g - T_{fc}$ is larger than that of the 0.3-mm thick Zr-BMG. Similarly, the $T_g - T_{fc}$ of 0.8-mm thick Zr-BMG is larger than that of the 0.6-mm thick Pd-BMG. Thus, $T_g - T_{fc}$ values measured for any sample size allow to predict the mechanical behaviour of different glass-forming alloys.

In summary, we propose $T_g - T_{fc}$ criterion to predict the room-temperature mechanical behaviour and its sensitivity to cooling rate and annealing-induced embrittlement for metallic glasses. We envision that application of structural models[40,41] can reveal the microscopic origin of such a critical fictive temperature to design tough metallic glasses.

Methods

Sample preparation. $Pt_{57.5}Cu_{14.7}Ni_{5.3}P_{22.5}$ and $Pd_{43}Cu_{27}Ni_{10}P_{20}$ alloys were prepared by induction melting the constituents in vacuum-sealed quartz tube. The alloys were subsequently fluxed with B_2O_3 at 1,000 °C for 600 s. The fluxed alloys were re-melted and water-quenched in 3-mm diameter quartz tubes to prepare the bulk amorphous samples. Amorphous $Zr_{44}Ti_{11}Cu_{10}Ni_{10}Be_{25}$ was acquired from Liquidmetal Technologies. Rectangular beams of 0.6 ± 0.05 mm thickness were machined from the bulk amorphous samples. To achieve the desired T_f, the beams were annealed at various temperatures (annealing temperature = T_f). Annealing times were chosen two times longer than the relaxation time, to ensure that the equilibrium had been reached at T_f. Crystallization can be ruled out, because the annealing times are at least an order of magnitude shorter than the crystallization times. After annealing, the samples were water-quenched to obtain the glassy state corresponding to different fictive temperatures.

Characterization. The samples were characterized thermally by DSC and structurally by X-ray diffraction. The glass transition temperature, T_g, was measured from DSC heating curves recorded at a heating with 20 K min^{-1}. Elastic constants were calculated from the shear and longitudinal sound velocities measured at room temperature by an ultrasonic technique. The bending strain to failure was measured by bending the beams around mandrels of different radii at room temperature[14]. The samples were mirror polished before the bending tests. The bending strain corresponds to $t/2r$ (t is the thickness of the samples and r is the radius of the mandrel). The average bending strain and error bars were calculated by testing five samples for each fictive temperature.

Construction of TTT diagrams for embrittlement. The samples were isothermally annealed at various temperatures followed by water quenching to room temperature. The embrittlement time corresponds to the annealing time for which the room-temperature bending strain to failure reduces to 2.5% or lower. TTT diagrams for embrittlement were constructed by plotting the log of isothermal embrittlement times as a function of temperature.

References

1. Greer, A. L. Metallic glasses. *Science* **267,** 1947–1953 (1995).
2. Inoue, A. Stabilization of metallic supercooled liquid and bulk amorphous alloys. *Acta Mater.* **48,** 279–306 (2000).
3. Johnson, W. L. Bulk glass-forming metallic alloys: science and technology. *MRS Bull.* **24,** 42–56 (1999).
4. Schuh, C. A., Hufnagel, T. C. & Ramamurty, U. Overview no. 144—mechanical behavior of amorphous alloys. *Acta Mater.* **55,** 4067–4109 (2007).
5. Xi, X. K. *et al.* Fracture of brittle metallic glasses: brittleness or plasticity. *Phys. Rev. Lett.* **94,** 125510 (2005).
6. Schroers, J. & Johnson, W. L. Ductile bulk metallic glass. *Phys. Rev. Lett.* **93,** 255506 (2004).
7. Liu, Y. H. *et al.* Super plastic bulk metallic glasses at room temperature. *Science* **315,** 1385–1388 (2007).
8. Demetriou, M. D. *et al.* A damage-tolerant glass. *Nat. Mater.* **10,** 123–128 (2011).
9. Lewandowski, J. J., Wang, W. H. & Greer, A. L. Intrinsic plasticity or brittleness of metallic glasses. *Phil. Mag. Lett.* **85,** 77–87 (2005).
10. Pauly, S., Gorantla, S., Wang, G., Kuhn, U. & Eckert, J. Transformation-mediated ductility in CuZr-based bulk metallic glasses. *Nat. Mater.* **9,** 473–477 (2010).
11. Zhang, L., Cheng, Y. Q., Cao, A. J., Xu, J. & Ma, E. Bulk metallic glasses with large plasticity: composition design from the structural perspective. *Acta. Mater.* **57,** 1154–1164 (2009).
12. Chen, M. W. Mechanical behavior of metallic glasses: microscopic understanding of strength and ductility. *Annu. Rev. Mater. Res.* **38,** 445–469 (2008).
13. Shen, J., Huang, Y. J. & Sun, J. F. Plasticity of a TiCu-based bulk metallic glass: effect of cooling rate. *J. Mater. Res.* **22,** 3067–3074 (2007).
14. Conner, R. D., Johnson, W. L., Paton, N. E. & Nix, W. D. Shear bands and cracking of metallic glass plates in bending. *J. Appl. Phys.* **94,** 904–911 (2003).
15. Volkert, C. A., Donohue, A. & Spaepen, F. Effect of sample size on deformation in amorphous metals. *J. Appl. Phys.* **103,** 083539 (2008).
16. Lu, J., Ravichandran, G. & Johnson, W. L. Deformation behavior of the $Zr_{41.2}Ti_{13.8}Cu_{12.5}Ni_{10}Be_{22.5}$ bulk metallic glass over a wide range of strain-rates and temperatures. *Acta Mater.* **51,** 3429–3443 (2003).
17. Raghavan, R., Murali, P. & Ramamurty, U. On factors influencing the ductile-to-brittle transition in a bulk metallic glass. *Acta Mater.* **57,** 3332–3340 (2009).
18. Kumar, G., Prades-Rodel, S., Blatter, A. & Schroers, J. Unusual brittle behavior of Pd-based bulk metallic glass. *Scripta Mater.* **65,** 585–587 (2011).
19. Das, J. *et al.* 'Work-hardenable' ductile bulk metallic glass. *Phys. Rev. Lett.* **94,** 205501 (2005).
20. Kumar, G., Ohkubo, T., Mukai, T. & Hono, K. Plasticity and microstructure of Zr-Cu-Al bulk metallic glasses. *Scripta Mater.* **57,** 173–176 (2007).
21. Castellero, A., Uhlenhaut, D. I., Moser, B. & Loffler, J. F. Critical Poisson ratio for room-temperature embrittlement of amorphous $Mg_{85}Cu_5Y_{10}$. *Phil. Mag. Lett.* **87,** 383–392 (2007).
22. Cheng, Y. Q., Cao, A. J. & Ma, E. Correlation between the elastic modulus and the intrinsic plastic behavior of metallic glasses: the roles of atomic configuration and alloy composition. *Acta Mater.* **57,** 3253–3267 (2009).
23. Kumar, G., Rector, D., Conner, R. D. & Schroers, J. Embrittlement of Zr-based bulk metallic glasses. *Acta Mater.* **57,** 3572–3583 (2009).
24. Madge, S. V., Louzguine-Luzgin, D. V., Lewandowski, J. J. & Greer, A. L. Toughness, extrinsic effects and Poisson's ratio of bulk metallic glasses. *Acta Mater.* **60,** 4800–4809 (2012).
25. Tandaiya, P., Ramamurty, U., Ravichandran, G. & Narasimhan, R. Effect of Poisson's ratio on crack tip fields and fracture behavior of metallic glasses. *Acta Mater.* **56,** 6077–6086 (2008).
26. Tool, A. Q. & Eichlin, C. G. Variations caused in the heating curves of glass by heat treatment. *J. Am. Ceram. Soc.* **14,** 276–308 (1931).
27. Geissberger, A. E. & Galeener, F. L. Raman studies of vitreous Sio2 versus fictive temperature. *Phys. Rev. B* **28,** 3266–3271 (1983).
28. Yue, Y. Z., von der Ohe, R. & Jensen, S. L. Fictive temperature, cooling rate, and viscosity of glasses. *J. Chem. Phys.* **120,** 8053–8059 (2004).
29. Lind, M. L., Duan, G. & Johnson, W. L. Isoconfigurational elastic constants and liquid fragility of a bulk metallic glass forming alloy. *Phys. Rev. Lett.* **97,** 015501 (2006).
30. Masuhr, A., Waniuk, T. A., Busch, R. & Johnson, W. L. Time scales for viscous flow, atomic transport, and crystallization in the liquid and supercooled liquid states of $Zr_{41.2}Ti_{13.8}Cu_{12.5}Ni_{10.0}Be_{22.5}$. *Phys. Rev. Lett.* **82,** 2290–2293 (1999).

31. Murali, P. & Ramamurty, U. Embrittlement of a bulk metallic glass due to sub-Tg annealing. *Acta Mater.* **53,** 1467–1478 (2005).
32. Deng, D. & Argon, A. S. Structural relaxation and embrittlement of $Cu_{59}Zr_{41}$ and $Fe_{80}b_{20}$ glasses. *Acta Metall. Mater.* **34,** 2011–2023 (1986).
33. Bohmer, R., Ngai, K. L., Angell, C. A. & Plazek, D. J. Nonexponential relaxations in strong and fragile glass formers. *J. Chem. Phys.* **99,** 4201–4209 (1993).
34. Legg, B. A., Schroers, J. & Busch, R. Thermodynamics, kinetics, and crystallization of $Pt_{57.3}Cu_{14.6}Ni_{5.3}P_{22.8}$ bulk metallic glass. *Acta Mater.* **55,** 1109–1116 (2007).
35. Lu, Z. P. & Liu, C. T. A new glass-forming ability criterion for bulk metallic glasses. *Acta Mater.* **50,** 3501–3512 (2002).
36. Moynihan, C. T., Easteal, A. J., Debolt, M. A. & Tucker, J. Dependence of fictive temperature of glass on cooling rate. *J. Am. Ceram. Soc.* **59,** 12–16 (1976).
37. Halpern, V. & Bisquert, J. The effect of the cooling rate on the fictive temperature in some model glassy systems. *J. Chem. Phys.* **114,** 9512–9517 (2001).
38. Kumar, G., Ohnuma, M., Furubayashi, T., Ohkubo, T. & Hono, K. Thermal embrittlement of Fe-based amorphous ribbons. *J. Non-Cryst. Solids* **354,** 882–888 (2008).
39. Badrinarayanan, P., Zheng, W., Li, Q. X. & Simon, S. L. The glass transition temperature versus the fictive temperature. *J. Non-Cryst. Solids* **353,** 2603–2612 (2007).
40. Miracle, D. B. A structural model for metallic glasses. *Nat. Mater.* **3,** 697–702 (2004).
41. Sheng, H. W., Luo, W. K., Alamgir, F. M., Bai, J. M. & Ma, E. Atomic packing and short-to-medium-range order in metallic glasses. *Nature* **439,** 419–425 (2006).

Acknowledgements

This work was funded by DOE, Office of Basics Energy Sciences through DE SC 0004889. We thank Sindee Simon and Dan Miracle for useful discussions.

Author contributions

G.K. and J.S. designed the study. G.K., P.N. and Y.L. conducted the experiments. G.K., P.N. and J.S. analysed the results and wrote the manuscript.

Additional information

Competing financial interests: The authors declare no competing financial interests.

Reprints and permission information is available online at http://npg.nature.com/reprintsandpermissions/

How to cite this article: Kumar, G. *et al.* Critical fictive temperature for plasticity in metallic glasses. *Nat. Commun.* 4:1536 doi: 10.1038/ncomms2546 (2013).

nature COMMUNICATIONS

DOI: 10.1038/ncomms3357

Corrigendum: Critical fictive temperature for plasticity in metallic glasses

Golden Kumar, Pascal Neibecker, Yan Hui Liu & Jan Schroers

Nature Communications 4:1536 doi: 10.1038/ncomms2546 (2013); Published 26 Feb 2013; Updated 17 Oct 2013

The funding for this Article was not fully acknowledged. The Acknowledgements should have read:

This work was funded by DOE, Office of Basics Energy Sciences through DE SC 0004889, and by the National Science Foundation through MRSEC DMR-1119826. We thank Sindee Simon and Dan Miracle for useful discussions.